RSC Advances

PAPER

View Article Online
View Journal | View Issue

Cite this: *RSC Adv.*, 2020, **10**, 8790

Insight into the synergistic effect on adsorption for Cr(VI) by a polypyrrole-based composite

Wanhong Sun, *[a] Wenbo Zhang,[b] Hailing Li,[a] Qiong Su,[bc] Ping Zhang[b] and Lihua Chen[b]

Received 25th October 2019
Accepted 10th February 2020

DOI: 10.1039/c9ra08756g

rsc.li/rsc-advances

Polypyrrole-based (PPy) composite are promising candidates for the treatment of water pollution. Adsorption selectivity as well as a large adsorption capacity are two key factors for treating wastewater containing multiple ions. The structure and morphology of the prepared composites were characterized by the FT-IR, XRD and SEM examinations. The results indicate that the Fe_3O_4 and PPy nanosphere coats attapulgite (ATP) closely and evenly. Herein, a novel Fe_3O_4 and ATP doped three-dimensional network structure PPy/Fe_3O_4/ATP composite was demonstrated as an excellent adsorbent to effectively remove Cr(VI). The as-synthesized PPy/Fe_3O_4/ATP composite is suitable for Cr(VI) adsorption in a wide pH range (pH 2–6). Up to a 96.44% removal rate was found with 400 mg L^{-1} Cr(VI) aqueous solution in 30 min for 0.2 g PPy/Fe_3O_4/ATP adsorbent. Adsorption results showed that Cr(VI) removal efficiency by PPy/Fe_3O_4/ATP decreased with an increase in pH. The removal rate of Cr(VI) had already reached 93.63% in 15 min contact time. Co-existing ions studies exhibit inorganic oxyacid anion and transition metal cation showed negative effects on Cr(VI) removal rate. A chemical rather than a physical adsorption occurred for these adsorbents as revealed by a pseudo-second-order kinetic study. The results of the adsorption isotherms showed that the adsorption process was similar to the Langmuir isotherm adsorption. Furthermore, the PPy/Fe_3O_4/ATP composite exhibited a high stability for Cr(VI) adsorption during recycling tests process. This work may provide some useful guidelines for designing adsorbents with selectivity toward specific heavy metal ions.

1. Introduction

Water pollution with heavy metal ions produced from the industry of mining, painting, car radiator manufacturing, batteries, and metal plating is increasingly becoming a significant environmental problem.[1] Chromium and its compounds, as an important raw material, are widely used in industrial production, but the discharged wastewater is one of the main sources of heavy metal pollution. A wide range of technologies have been employed to remove chromium and its compounds from wastewater to eliminate their effects on the environment.[2] Adsorption is believed to be an effective, economically viable, environmentally friendly and cost-effective technique for removing Cr(VI) from wastewater.[3] Therefore, in addition to the large adsorption capacity, the selective adsorption ability of the adsorbent is especially important in the treatment of wastewater.[4]

It was found that the synergistic effect introduced by the two nanosized fillers may play an important role. Magnetic materials (Ni, Co, *etc.*) and ferrites (Fe_3O_4, α-Fe_2O_3, *etc.*) have been widely utilized as nanosized fillers in matrices to fabricate sewage treatment absorbents.[5] And that magnetic materials exhibit the advantages including the reduction of secondary pollution, ease of separation, and high adsorption capacity.[6] Attapulgite (ATP) is a kind of crystalline hydrated magnesium aluminum silicate with unique fibrous three-dimensional structure, excellent chemical stability and strong adsorption.[7,8] However, ATP may easily agglomerate due to its large surface area, and therefore its adsorption efficiency becomes low.

Nanostructured adsorbents based on a conductive polymer have emerged as strong candidates for the removal of various heavy metal ions, such as Hg(II),[9] Cr(VI),[2–4] Ni(II),[10] Pb(II),[11,12] Cu(II),[1] Zn(II),[13] and V(V)[14] due to their high chemical stability and nontoxicity. Further, high affinity by functionalized conducting PPy composite is a reliable approach to enhance the accumulation of target metal ions. Due to its redox property, PPy is especially suitable for the remediation processing of Cr(VI). For examples, the multiwalled carbon nanotube (MWCNT) modified carbon cloth (CC) was used as carrier for electrodepositing PPy to synthesize CC-MWCNT-PPy adsorbent for Cr(VI).[15] Fang *et al.*[16] synthesized graphene/SiO_2@PPy

[a]*Department of Experimental Teaching, Northwest Minzu University, Lanzhou, 730030, P. R. China. E-mail: sunwh2004@126.com*

[b]*School of Chemical Engineering, Northwest Minzu University, Lanzhou, 730030, P. R. China*

[c]*Key Laboratory of Environmental Friendly Composite Materials and Biomass Utility in Universities of Gansu Province, Northwest Minzu University, Lanzhou, 730030, P. R. China*

composites, which showed a maximum adsorption capacity of 429.2 mg g^{-1} for Cr(VI). Yang *et al.*[17] reported the magnetic corncob biochar/PPy material with adsorption capacity of 19.23 mg g^{-1}. The PPy/ATP were utilized as adsorbent for the removal of Cr(VI), which showed a maximum adsorption capacity of 46.14 mg g^{-1}.[8] Specifically, conjugated PPy is a promising candidate due to its novel conjugated structure and redox properties, offering a rich electrochemical chain that undergoes ion doping and dedoping on the PPy nitrogen, which may additionally experience interaction and synergistic effect with metal oxides.[18]

Inspired by the above analysis and based on our previous work of PPy-based composites.[19,20] In this work, the three-dimensional network structure composite with PPy and Fe_3O_4 on the ATP surface were synthesized, characterized, and evaluated as an adsorbent for removing Cr(VI) from aqueous solution by batch adsorption experiments.

2. Material and methods

2.1 Materials

Pyrrole (Py, 99%, Shanghai Chemical Company, China) was purified by vacuum distillation and stored in refrigerator prior to use. ATP was supplied by Jiangsu Xuyi. Iron(III) chloride hexahydrate, ferrous sulfate heptahydrate, ethyl alcohol, sodium hydroxide, hydrochloric acid, ammonia hydroxide, sulfuric acid, *p*-toluenesulfonic, dodecyl benzene sulfonic acid sodium (SDBS), acetone and potassium dichromate ($K_2Cr_2O_7$) were obtained from commercial suppliers and used as received. All chemicals were of reagent grade.

2.2 Preparation of Fe_3O_4 nanoparticles

The Fe_3O_4 magnetic nanoparticles were synthesized through a coprecipitation method according to previous reports.[21] The synthetic process was as follows: 0.1 mol L^{-1} $FeCl_3 \cdot 6H_2O$ and 0.05 mol L^{-1} $FeSO_4 \cdot 7H_2O$ with the same volume were kept sufficiently stirring after mixing in a round bottom flask. Then 1.5 mol L^{-1} 30 mL ammonia hydroxide was added slowly into the mixture to adjust the pH value to 9–10. The mixture was stirred at 80 °C for 2 h. The black precipitate was collected by magnet and washed with deionized water until the pH of the supernatant was neutral. The powders were dried overnight in a 50 °C vacuum oven to obtain the magnetic nanoparticles.

2.3 Activation process of ATP

The activation process of ATP was as follows: 0.5 g attapulgite and 50 mL 2 mol L^{-1} HCl were added to a round bottom flask. The mixture was stirred at room temperature for 4 h and rinsed for several times with deionized water and anhydrous ethanol until the filtrate was neutral, and dried at 50 °C in vacuum for 24 h.

2.4 Preparation of PPy/Fe_3O_4/ATP

As the preparation of PPy/Fe_3O_4/ATP composite, 0.2 mg SDBS and 30 mL ethyl alcohol–water (1 : 1) were mixed and sonicated for 15–20 min at room temperature. Then 0.4 g of Fe_3O_4 and ATP treated with hydrochloric acid was injected into the above mixture and sonicated for 60 min. 1.1 mL of pyrrole and 0.45 g of *p*-toluene sulfonic acid were added into the above mixture and sonicated for 15 min under 0–5 °C. Finally, 50 mL 0.9 mol L^{-1} $FeCl_3 \cdot 6H_2O$ aqueous solution was added slowly into the reactor and a rapid oxidation occurred. The resulted suspension was sonicated at 0–5 °C for 2 h. The polymerization was allowed to proceed about 16 h at room temperature in the rotatory shaker. The obtained products were filtered or separated by magnet and washed with deionized water and ethanol, and dried at 50 °C in vacuum for 24 h.

2.5 Characterization

Fourier-transform infrared spectra (FT-IR) of the samples in KBr pellets were recorded on an EQUINOX55 FT-IR spectrometer (Bruker). X-ray diffraction studies were performed by using D/max-2400 diffraction X-ray diffractometer (Rigaku) with CuKα as radiation source. Scanning electron microscope (SEM, Hitachi, Japan, JEOL, JSM-6330F) was used to observe the morphologies of composite. Prior to the examination, the specimens were coated with a very thin layer of gold.

2.6 Batch experimental procedures

$K_2Cr_2O_7$ was used as the source of Cr(VI) simulate waste. The Cr(VI) aqueous solutions were prepared by mixing $K_2Cr_2O_7$ in water and diluted with deionized water to form a series of desired concentrations. The pH values of solution in these experiments were approximately 2, 3, 4, 5.6, 8 and 9. The pH value was adjusted by 0.1 mol L^{-1} H_2SO_4 and 0.1 mol L^{-1} NaOH solution. The initial concentration of Cr(VI) was 100, 200, 300, 400, 500 and 700 mg L^{-1} respectively. The dose of adsorbate was 50, 100, 150, 200 and 250 mg respectively. The contact time of adsorption process was 5, 15, 30, 60 and 180 min respectively. For determining the amount of Cr(VI) removal by samples, 0.2 g PPy/Fe_3O_4/ATP was added into 20 mL of Cr(VI) ions solution with scheduled concentration and strongly shaken at a rate of 160 rpm in an oscillator to ensure a complete mixing. At the end of predetermined time intervals, the samples were filtered or separated by magnet and the concentration of Cr(VI) was determined using a UV-visible spectrometer at 540 nm according to diphenylcarbazide method. All adsorption experiments were conducted at 20 ± 2 °C unless noted, and all of the adsorption results were corrected by blank tests in which no adsorbent was added into the Cr(VI) solution. All experiments were carried out twice and the adsorbed concentrations given were the means of duplicate experimental results.

Adsorption equilibrium experiments were carried out in a temperature controlled thermostatic shaker operated at 160 rpm. All the Cr(VI) solutions required for experiments were freshly prepared by diluting the stock solution. The removal rate of Cr(VI) and the adsorption capacity q_t (mg g^{-1}) were calculated by eqn (1) and (2).

$$\text{Removal rate } (\%) = [\,(c_0 - c_t)/c_0] \times 100\% \quad (1)$$

$$q_t = [V \times (c_0 - c_t)]/m \quad (2)$$

where c_0 and c_t (mg L^{-1}) are the initial and time t concentrations of Cr(VI), respectively. V was the solution volume (mL) and m was the mass of PPy/Fe_3O_4/ATP adsorbent (g).

2.7 Adsorption kinetics experiments

For the kinetics study, 20 mL of Cr(VI) solution (400 mg L^{-1}) at pH 2 containing 20 mg of PPy/Fe_3O_4/ATP was placed in an oscillator and agitated at 160 rpm for different contact times (20 °C). At a predetermined time interval (0–180 min), the Cr(VI) solution was filtered or separated by magnet, collected, and used for analyzing Cr(VI) concentration. The adsorption capacity of the PPy/Fe_3O_4/ATP q_t (mg g^{-1}) at time t was obtained from eqn (2).

2.8 Sorption isotherms experiments

In the isotherm investigations, the PPy/Fe_3O_4/ATP was dosed in Cr(VI) solutions of various initial concentrations (100, 200, 300, 400, 500 mg L^{-1}) for 30 min at 20 °C. The procedure was similar to that described for the effect of initial concentration of Cr(VI).

2.9 Regeneration experiments

Adsorption–desorption experiments were carried out to regenerate the PPy/Fe_3O_4/ATP after adsorbing Cr(VI) for further use. Initially, saturated adsorbent was added into 0.5 mol L^{-1} NaOH solution for shaking 24 h with the dosage of 0.2 g L^{-1} at room temperature. Thereafter, the PPy/Fe_3O_4/ATP was put into 1.0 mol L^{-1} HCl solution for 0.5 h to regenerate the adsorption sites and rinsed with distilled water to neutral. And above two steps was repeated several times for the adsorbent regeneration.[22]

3. Results and discussion

3.1 Structure and morphology

Fig. 1a shows the FT-IR spectra of the bare PPy, Fe_3O_4, ATP and PPy/Fe_3O_4/ATP composite. The spectrum of the PPy showed the typical absorbance peaks at 1548 and 1456 cm^{-1} corresponding to the symmetric and antisymmetric stretching modes of the PPy ring, respectively.[9,23] The peak at 1170 cm^{-1} is assigned to C–C stretching. The band at 1042 and 907 cm^{-1} is due to in-plane deformation of C–H bond of pyrrole ring.[24] The characteristic peak of Fe_3O_4 at 470 cm^{-1} is for the stretching vibration of Fe–O bond according to reports.[25] It can be seen from ATP spectra that the peaks at 1086 cm^{-1}, 791 cm^{-1} and 565 cm^{-1} are respectively attributed to Si–O–Si stretching vibration and bending vibration.[8] After polymerization, the spectrum of PPy/Fe_3O_4/ATP composite clearly exhibits characteristic absorption peaks with respect to PPy, Fe_3O_4, ATP, which indicates the formation of PPy/Fe_3O_4/ATP composite.

The phase purity and crystal structure of the samples have been identified by X-ray diffraction technique and the results are shown in Fig. 1b. The PPy in $2\theta = 20$–$30°$ has a broad peak, and the absorption peak located at 23.52° is obvious, which is the characteristic peaks of pure PPy.[26] It can be clearly seen that almost all the diffraction peaks of Fe_3O_4 can be assigned to the cubic Fe_3O_4 (JCPDS 88-0866), the peaks at 30.22°, 35.56°, 43.25°, 53.53°, 57.20°, 62.81° can be indexed to (220), (311), (400), (422), (511), (440) crystal planes of cubic Fe_3O_4, respectively.[8] The XRD pattern of ATP shows that the peak positions (2θ = 19.80°, 27.49°, 34.6° and 42.5°) are the characteristic peak. By comparing the XRD patterns, there is the scattering peaks of PPy, Fe_3O_4, ATP samples in the XRD pattern of PPy/Fe_3O_4/ATP composite, which demonstrates that the PPy, Fe_3O_4, ATP still exists in PPy/Fe_3O_4/ATP composite.

The morphology of the fabricated three-dimensional composite was observed by SEM, as shown in Fig. 2. Fig. 2a shows the spherical morphology of the prepared PPy with an average diameter is about 100 nm. It can be clearly seen from Fig. 2b that the shape of the Fe_3O_4 prepared in this experiment is spherical nanoparticle with agglomeration phenomenon. It can be found that APT is rod-like in shape with a length of 0.5–1.5 μm and a diameter of 30–120 nm (Fig. 2c). In Fig. 2d, it can be found that the prepared PPy/Fe_3O_4/ATP exhibits a three-dimensional network structure with an average pore diameter of about several to tens of micrometers. The PPy nanosphere and PPy/Fe_3O_4 core–shell nanosphere coated with PPy on the Fe_3O_4 surface are uniformly attached on the surface of ATP, which is helpful to avoid the aggregation of PPy, Fe_3O_4 and ATP in the *situ* oxidation polymerization process (Fig. 2d).[27] Compared with the smooth surface of APT (Fig. 2c), PPy/Fe_3O_4/ATP composite show a coarse surface (Fig. 2d). The three-

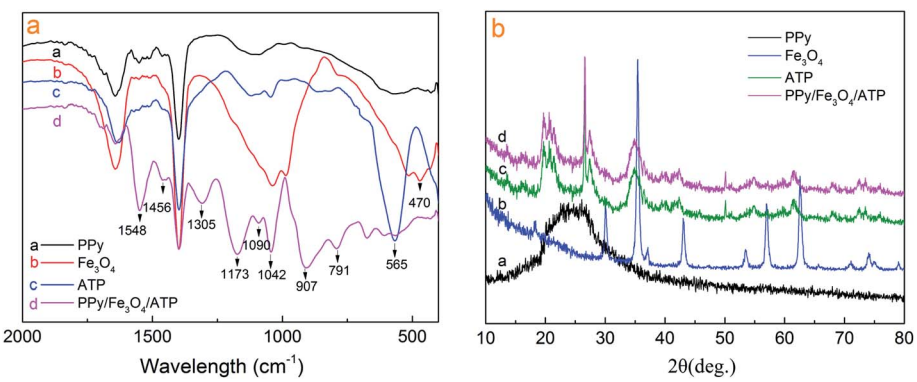

Fig. 1 IR (a) and XRD (b) spectra of PPy, Fe_3O_4, ATP and PPy/Fe_3O_4/ATP composite.

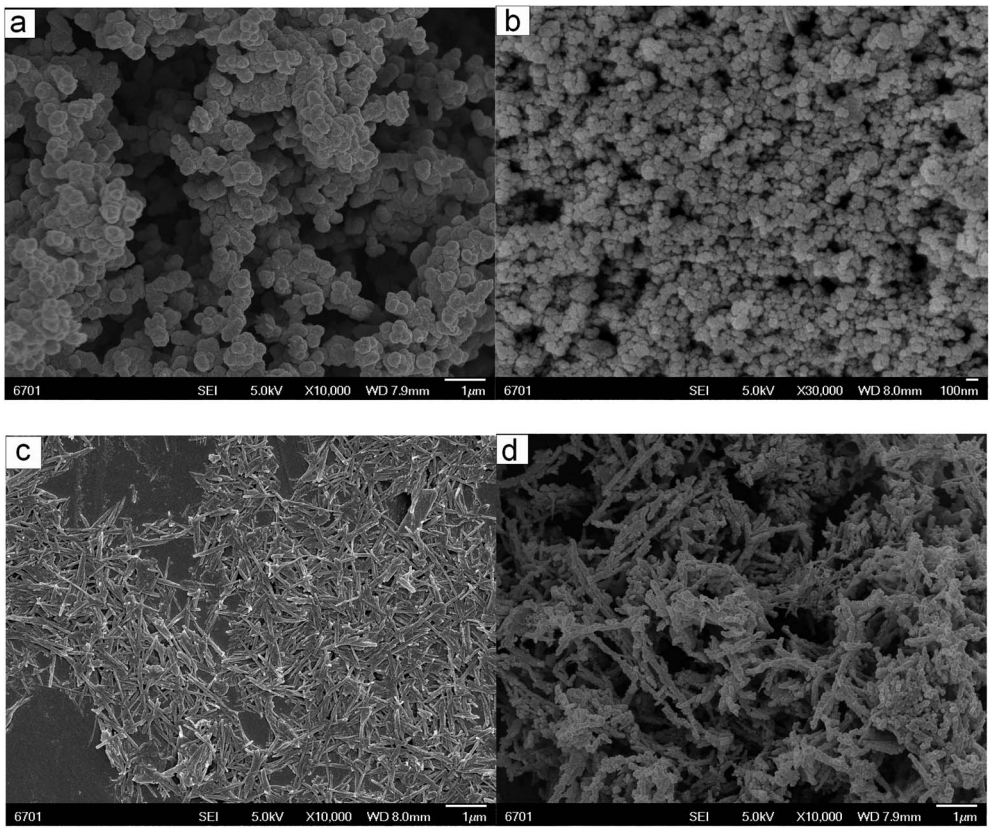

Fig. 2 SEM micrographs of PPy (a), Fe_3O_4 (b), ATP (c) and PPy/Fe_3O_4/ATP (d) composite.

dimensional network structure, the uniform distribution of PPy, Fe_3O_4 and ATP and coarse surface can be favorable for the Cr(VI) absorption behavior.[2] The high specific surface area and three-dimensional network interconnected composite are capable of the pollutant removal from wastewater.[9]

3.2 Adsorption performance of PPy/Fe_3O_4/ATP composite

It is well known that the conductive polymer containing amine or imine functional group can adsorb some matters from waste water.[19,25] Magnetic Fe_3O_4 plays two fold roles: it adsorbs Cr(VI) ions and is important for imparting magnetic property to the PPy/Fe_3O_4/ATP.[4,5] Therefore, the as-prepared PPy/Fe_3O_4/ATP composite is suitable as an efficient adsorbent for removal of Cr(VI) from the waster water.

The solution pH is an important controlling parameter in the adsorption process which is responsible for the adsorbent surface charge and the degree of ionization.[2,3] Consequently, for the treatment of Cr(VI)-contaminated wastewater with PPy/Fe_3O_4/ATP composite, the initial pH may influence the performance of the composite. Fig. 3a illustrates the influence of solution pH on the removal of Cr(VI) using PPy/Fe_3O_4/ATP as adsorbent at different pH conditions ranged from 2 to 9. It can be seen from Fig. 3a that the removal of Cr(VI) decreased with the increase in pH and the maximum removal of the Cr(VI) was occurred at pH 2. The higher removal percentage of the Cr(VI) in the pH range of 2–6 is due to the anion exchange of PPy/Fe_3O_4/ATP composite by replacing the doped Cl^- ions with either $HCrO_4^-$ or $Cr_2O_7^{2-}$ ions. Meanwhile, the –NH group present in the PPy matrix may also get protonated and it electrostatically attracts the anionic $HCrO_4^-$ ions.[2,28] However, with the pH values increasing, the number of hydroxyl (OH^-) in the solution also increases, leading to the competitive interaction between CrO_4^{2-} and OH^- for the limited adsorption sites. As a result, the removal efficiency of Cr(VI) declines.

The effect of initial Cr(VI) concentration was investigated at different Cr(VI) concentrations (100–700 mg L^{-1}). As shown by PPy/Fe_3O_4/ATP adsorption curves (Fig. 3b), the Cr(VI) equilibrium concentration increased with the increase of initial Cr(VI) concentration. Apparently, adsorption was a passive process driven by concentration gradient as a driving force.[29] Fig. 3b showed that the removal of Cr(VI) gradually decreases with the increase of Cr(VI) solution concentration. When the initial Cr(VI) concentration is 100 mg L^{-1}, the removal rate of Cr(VI) was as high as 99.84% and the Cr(VI) ions in the solution are almost completely adsorbed by PPy/Fe_3O_4/ATP composites. However, the removal rate of Cr(VI) was only 52.48% with the Cr(VI) concentration of 700 mg L^{-1}. Only half of the Cr(VI) ions have been removed. The reason might that the total available adsorption sites were limited at a fixed adsorbent dosage, which became saturated at a higher Cr(VI) concentration.[30]

The effect of PPy/Fe_3O_4/ATP composite dosage on the removal of Cr(VI) from aqueous solution was shown in Fig. 3c. The removal efficiency increased from 29.91% to 99.92% with an increase of dosage from 0.05 g to 0.25 g, which could be

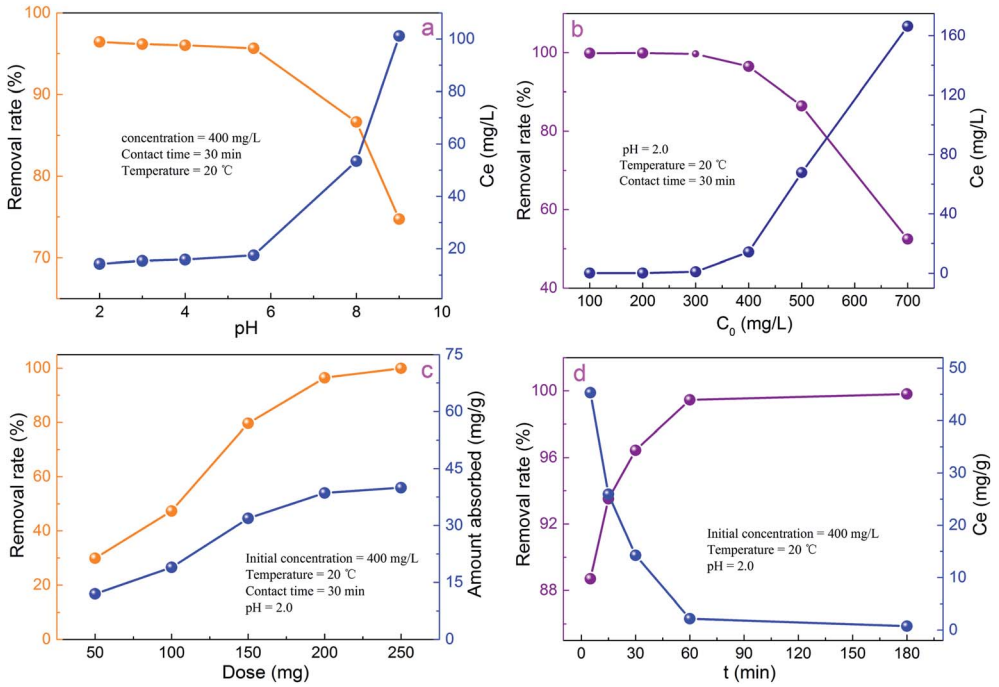

Fig. 3 Effect of pH (a), initial concentration (b), dose (c) and contact time (d) on the Cr(VI) removal of the PPy/Fe_3O_4/ATP composite.

attributed to an increase in surface area and availability of more active adsorption sites for Cr(VI).[17] On the other hand, the amount adsorbed was about 39.97 mg g^{-1} for the adsorbent dose of 0.25 g, indicating maximum adsorption capacity at 0.25 g. Considering the removal efficiency and cost benefit, an adsorbent dosage of 0.2 g, the minimum dosage required for complete removal of Cr(VI) from 400 mg L^{-1} Cr(VI) solution, was used for subsequent adsorption experiments.

To discuss the influence of contact time on the removal of PPy/Fe_3O_4/ATP composite, a series of experiments were carried out at 20 °C from 5–180 min. Fig. 3d demonstrates that the removal rate of Cr(VI) clearly increases with the increase contact time. The removal rate of Cr(VI) had already reached 93.52% in 15 min contact time. The PPy/Fe_3O_4/ATP composite completely removes Cr(VI) from the aqueous solution in 60 min, and the Cr(VI) removal efficiency reaches up to 99.46%. This suggests that the most of the adsorption sites of the adsorbent existed in the exterior of the PPy/Fe_3O_4/ATP composites and were easily accessible by the Cr(VI) ions, resulting in a rapid process to adsorption equilibrium. The rapid adsorption for Cr(VI) using PPy/Fe_3O_4/ATP as adsorbent may be attributed to the synergistic effect of PPy, Fe_3O_4 and ATP.[8,31] This also indicates that the PPy/Fe_3O_4/ATP composites is particularly suitable for Cr(VI) adsorbents.

Usually, the constitution of industrial wastewater is complicated, containing multiple anions and cations, such as NO_3^-, SO_4^{2-}, F^-, Cl^-, Cu^{2+}, Zn^{2+}, Ni^{2+}, Mg^{2+} and Na^+. Co-existing ions might compete with Cr(VI) for the adsorption sites on the adsorbents. So, some typical anions and cations were added into the reaction solution to estimate its effects on Cr(VI) adsorption. The initial concentrations of Cr(VI) were 400 mg L^{-1} and the pH was 2.0. As shown in Fig. 4a and b, these anions and cations with the concentration increase (15–60 mg L^{-1}) would have different effects on the Cr(VI) removal. It was observed clearly that the Na^+ had slightly affection Cr(VI) removal. NO_3^-, SO_4^{2-}, Fe^{3+}, Ni^{2+} and Zn^{2+} showed negative effects on Cr(VI) removal rate. The reduction shown in Cr(VI) removal could be attributed to the competition for the same active sites of adsorption and ion charge, size and concentration of the anions and cations.[28] Tang *et al.*[32] concluded that the ratio of charge towards radius (z/r) of the anion was closely correlated with their affinity to the adsorbent. The z/r values of these anions are in the order of CO_3^{2-} > SO_4^{2-} > NO_3^- > Cl^-. The higher z/r led to stronger interaction between the anions and the adsorption sites. Hence, the effect of these ions on Cr(VI) removal was in the order of SO_4^{2-} > NO_3^- > F^- > Cl^-.[32] This order was consistent with that of our experiment. Thus, the effect of coexisting cations on Cr(VI) removal is estimated to be similar.

3.3 Possible adsorption mechanism

The synthesis process of PPy/Fe_3O_4/ATP composite and possible mechanism of Cr(VI) removal is shown in Scheme 1. There are several plausible mechanisms for Cr(VI) adsorption using a green-multifunctional adsorbent including ion exchange, electric attraction, reduction reaction, and metal chelate complex processes.[3,9,33] The Cr(VI) mainly exists as $Cr_2O_7^{2-}$ and $HCrO_4^-$ with pH in the range 2–6. The removal of Cr(VI) by the PPy/Fe_3O_4/ATP composite maybe occurred through ion exchange, replacing the doped Cl^- with $Cr_2O_7^{2-}$ or $HCrO_4^-$, and electrostatic interaction between positively charged nitrogen (N^+) and $Cr_2O_7^{2-}$ or $HCrO_4^-$.[16,17] At pH 2, the PPy/Fe_3O_4/ATP

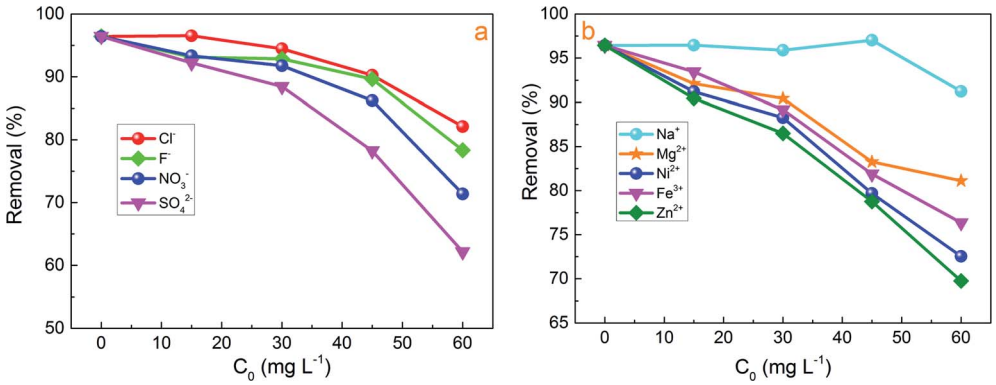

Fig. 4 The effect of co-existing ions on the adsorption of Cr(VI).

composite is positively charged and highly protonated, the positively charged nitrogen (N^+) acts as the active sites to adsorb $Cr_2O_7^{2-}$ or $HCrO_4^-$.[27] According to previous research, the positive $-NH^+$ group in a polymer chain possessed a capacity for reduction. So the $Cr_2O_7^{2-}$ and $HCrO_4^-$ was reduced to Cr(III) according to the following two equations:[34]

$$HCrO_4^- + 7H^+ + 3e \rightarrow Cr^{3+} + 4H_2O \quad (3)$$

$$Cr_2O_7^{2-} + 14H^+ + 6e \rightarrow 2Cr^{3+} + 4H_2O \quad (4)$$

The reduction process had occurred on the surface of PPy/Fe_3O_4/ATP composite during the Cr(VI) adsorption, a considerable part of the Cr(VI) is reduced to Cr(III) by the electron-rich amino group of PPy due to reversible transformation between the present state (PPy^0) and the oxidative state (PPy^+) under an acidic environment.[16] Furthermore, Cr(III) ions likely forms a coordination compound with hydroxyl on the ATP. Therefore, hydroxyl on the ATP contribute their one pair of electrons to Cr(III) for strong soft acid–base interactions shown in Scheme 1.

3.4 Adsorption kinetics

Fig. 5 illustrates the adsorption capacity of Cr(VI) adsorbed by prepared adsorbents with the passage of the contact time (0–90 min). The amount of adsorbed Cr(VI) rapidly increased with time and then plateaued to equilibrium for PPy/Fe_3O_4/ATP adsorbents. To understand the kinetic mechanism of the present adsorption process, pseudo-first-order and pseudo-second-order models were used to fit the kinetic data. The linear forms of the pseudo-first-order and pseudo-second-order equations are given in eqn (5) and (6), respectively:[35,36]

$$\log(q_e - q_t) = \log q_e - \left(\frac{k_1}{2.303}\right) \times t \quad (5)$$

$$\frac{t}{q_t} = \frac{1}{k_2 q_e^2} + \frac{t}{q_e} \quad (6)$$

where q_t (mg g^{-1}) is the adsorption capacity at time t, k_1 (min^{-1}) is the rate constant of the pseudo-first-order equation, and k_2 (g (mg $min)^{-1}$) is the rate constant of the pseudo-second-order equation.

The linearized plots of eqn (3) and (4) are separately shown in Fig. 5a and b. The determined values for the corresponding parameters of the kinetic models are presented in Table 1. From the values of the correlation coefficients, the pseudo-second-order model ($R^2 = 0.9999$) gave a better description of the Cr(VI) adsorption compared to the pseudo-first-order model ($R^2 = 0.9968$), which indicates that the rate-limiting step might be the chemical adsorption. Moreover, the q_{cal} values (40.00 mg g^{-1})

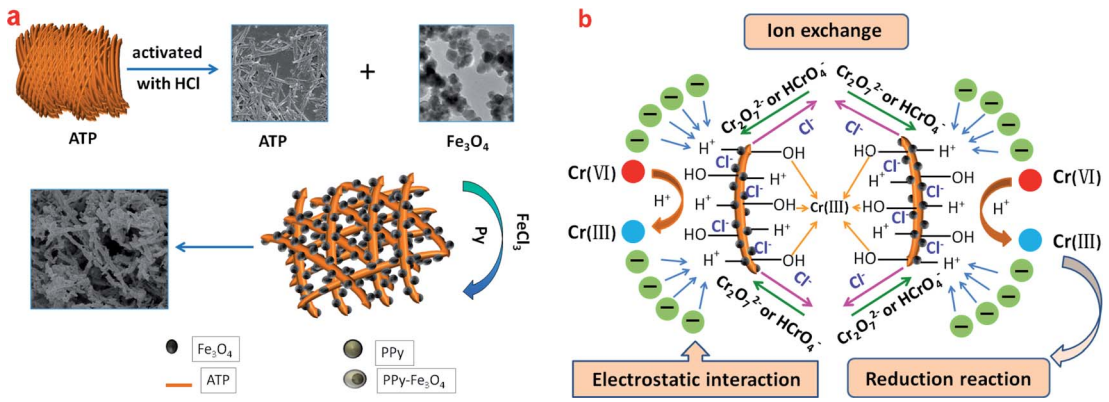

Scheme 1 Preparation process of PPy/Fe_3O_4/ATP composite (a) and mechanism of Cr(VI) removal (b).

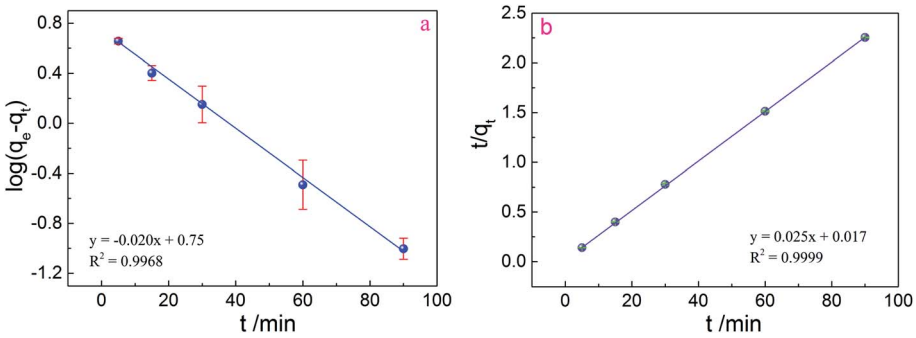

Fig. 5 Kinetic fitting plots of pseudo-first-order (a) and pseudo-second-order (b) equations.

Table 1 Comparison of pseudo-first-order and pseudo-second-order adsorption rate constants and adsorption capacities

First-order rate constant			Second-order rate constant		
k_1 (min^{-1})	q_e (mg g^{-1})	R^2	k_2 g (mg min)$^{-1}$	q_e (mg g^{-1})	R^2
0.046	5.62	0.9968	0.036	40.00	0.9999

obtained by pseudo-second-order model were closer to the experimental data (53.37 mg g^{-1}), indicating that the pseudo-second-order kinetic model could better describe the removal process of Cr(VI) by PPy/Fe_3O_4/ATP composite. It might be suggested that the rate of Cr(VI) removal was dependent on the availability of active adsorption sites rather than the concentration of adsorbate.[17]

3.5 Adsorption isotherm

Equilibrium adsorption isotherm data are important to properly operate an adsorption system and investigate the capacity of PPy/Fe_3O_4/ATP composite for adsorption of Cr(VI). The Freundlich model describes the relationship between adsorbent and adsorbate, usually the ratio of the quantity absorbed and remained in the solution at equilibrium at a fixed temperature.[35] Fig. 6 depicts the equilibrium adsorption isotherm data for Cr(VI) adsorption by PPy/Fe_3O_4/ATP composite at temperatures 20 °C. The Langmuir model is used to describe the adsorption on a homogeneous and flat surface of an adsorbent, and each adsorptive site could be occupied only once in a one-on-one manner. On the other hand, the Freundlich isotherm model is an empirical equation valid for the adsorption of a reversible heterogeneous surface.[37] Two adsorption kinetic models can be described as eqn (7) and (8):

$$\frac{c_e}{q_e} = \frac{1}{bq_{max}} + \frac{c_e}{q_{max}} \quad (7)$$

$$\log q_e = \log K_f + 1/n \log c_e \quad (8)$$

where c_e (mg L^{-1}) is the equilibrium concentration of Cr(VI) in water, q_e (mg g^{-1}) is the Cr(VI) amount adsorbed at equilibrium, q_{max} (mg g^{-1}) is the amount adsorbed onto the surface of adsorbent at equilibrium. The value of b (L mg^{-1}) relates the heat of adsorption, while the Langmuir constants q_{max} represent the adsorption capacity of monolayer adsorbent. K_f is the Freundlich equilibrium constant, and n is an experimental parameter which describe the intensity of adsorption related with heterogeneity of the adsorbent surface. The adsorption is considered as favorable if the value of $1/n$ lies in between 0 and 1.[29]

The adsorption capacities of the as-obtained PPy/Fe_3O_4/ATP to Cr(VI) were measured individually at pH 2.0 with 0.2 g of PPy/Fe_3O_4/ATP and varied Cr(VI) concentration. The relative parameters calculated from the two models are listed in Table 2. With higher R^2 values, the Langmuir model (R^2 = 0.9803) can better reflect the isotherm characteristics of the adsorption process than the Freundlich model (R^2 = 0.6297), suggesting that the surface of the PPy/Fe_3O_4/ATP composite

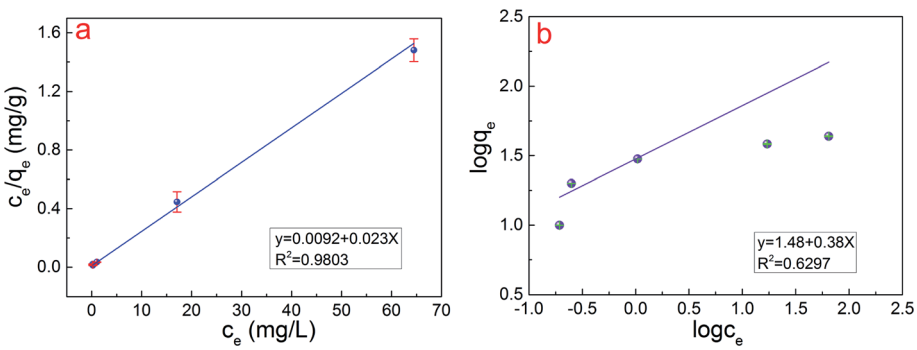

Fig. 6 (a) Langmuir and (b) Freundlich isotherms for Cr(VI) removal by PPy/Fe_3O_4/ATP composite.

Table 2 Isotherm parameters for the adsorption of Cr(VI) on PPy/Fe_3O_4/ATP composite

Langmuir model			Freundlich model		
q_{cal} (mg g^{-1})	b (L mg^{-1})	R^2	K_f	n	R^2
43.48	2.5	0.9803	30.20	2.63	0.6297

was homogenous and the monolayer adsorption was the main adsorption mechanism for Cr(VI).[17] The values of $1/n$ obtained in this study were between 0.38. The closer the values of $1/n$ towards 1, the better the favorability of adsorption is, which indicated a unfavorable adsorption process for the Freundlich model.[29] The maximum adsorption capacity (q_{exp}) in the experiment is 53.37 mg g^{-1} as Fig. 3b shows, which is also consistent with the Langmuir model (q_{cal}, 43.48 mg g^{-1}).

3.6 Regeneration experiment

Adsorption–desorption experiments were carried out to regenerate the PPy/Fe_3O_4/ATP composite after adsorbing Cr(VI) for further use. As Fig. 7 shown, the removal rate of PPy/Fe_3O_4/ATP remained about 82.79% for the two cycles and in the subsequent fourth cycle the removal rate decreased to 64.1%. As the number of adsorption cycles increases, the decrease of Cr(VI) removal can be attributed to the consumption of the PPy/Fe_3O_4/ATP composite and the blocked active sites by the adsorbed Cr(VI) and Cr(III).[38] However, the removal was still higher than 60% after the four adsorption–desorption processes, possibly due to the formation of stable network of PPy/Fe_3O_4/ATP composite.[39]

The low cost of the separation and regeneration of a material is critical for its application as an adsorbent and will make the adsorbent in large-scale application. In our absorption experiment, the PPy/Fe_3O_4/ATP was separated from the solution with the external magnetic field, and this separation process could be finish quickly.[25,40] Furthermore, the PPy/Fe_3O_4/ATP composite was regenerated by simple operation, low cost and efficiency.[4,41]

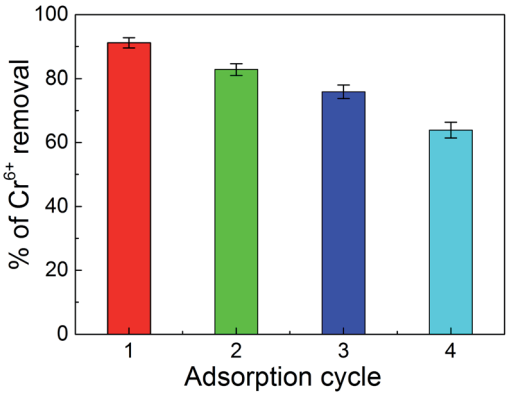

Fig. 7 Desorption and regeneration of PPy/Fe_3O_4/ATP composite.

4. Conclusion

In this study, chemical oxidative polymerization method was used to prepare PPy/Fe_3O_4/ATP composite by coating the ATP surface with PPy/Fe_3O_4 and PPy and their ability in the removal of Cr(VI) from wastewater was investigated. Adsorption capacity of Cr(VI) much depend on pH of solutions and the best results are obtained at the pH range from 2–6. Adsorption equilibrium is attained within a short contact time of 30 min when the initial Cr(VI) concentration was 400 mg L^{-1}. The presence of co-existing ions, including NO_3^-, SO_4^{2-}, Fe^{3+}, Ni^{2+} and Zn^{2+}, had no significant influence on removing Cr(VI) for low concentrations of coexisting ions. Batch adsorption experiment shows that experimental data were well fitted with pseudo-second-order kinetic model and Langmuir model, suggesting that the adsorption process might be chemisorption and occur on the surface of PPy/Fe_3O_4/ATP by a monolayer adsorption. Adsorption capacity calculated according to the Langmuir isotherm was 53.37 mg g^{-1} at an initial pH of 2.0 for the 400 mg L^{-1} Cr(VI) solution. There are several plausible mechanisms for Cr(VI) adsorption including ion exchange, electric attraction, reduction reaction, and metal chelate complex processes. The PPy/Fe_3O_4/ATP composite can be easily regenerated and reused for Cr(VI) adsorption several times with good efficiency and high durability.

Conflicts of interest

There are no conflicts to declare.

Acknowledgements

The authors would like to thank the financial supported by Funds of Central Universities Fundamental Research (31920190049), supported by fund of the National Natural Science Foundation of China (21968032), supported by fund of the Fundamental Research Funds of Central Universities-Innovation Team Cultivation Project (31920190012).

References

1 J. Chen, M. Yu, C. Wang, J. Feng and W. Yan, Insight into the synergistic effect on selective adsorption for heavy metal ions by a polypyrrole/TiO_2 composite, *Langmuir*, 2018, **34**, 10187–10196.
2 Y. Lei, X. Qian, J. Shen and X. An, Integrated reductive/adsorptive detoxification of Cr(VI)-contaminated water by polypyrrole/cellulose fiber composite, *Ind. Eng. Chem. Res.*, 2012, **51**, 10408–10415.
3 Q. Zhou, J. Huang, X. Zhang and Y. Gao, Assembling polypyrrole coated sepiolite fiber as efficient particle adsorbent for chromium(VI) removal with the feature of convenient recycling, *Appl. Clay Sci.*, 2018, **166**, 307–317.
4 A. M. Muliwa, T. Y. Leswifi, M. S. Onyango and A. Maity, Magnetic adsorption separation (MAS) process: an alternative method of extracting Cr(VI) from aqueous

solution using polypyrrole coated Fe_3O_4 nanocomposite, *Sep. Purif. Technol.*, 2016, **158**, 250–258.

5 Z. Wu, D. Tan, K. Tian, W. Hu, J. Wang and M. Su, Facile preparation of core-shell Fe_3O_4@polypyrrole composite with superior electromagnetic wave absorption properties, *J. Phys. Chem. C*, 2017, **121**, 15784–15792.

6 G. Chen, C. Qiao, Y. Wang and J. Yao, Synthesis of magnetic gelatin and its adsorption property for Cr(VI), *Ind. Eng. Chem. Res.*, 2014, **53**, 15576–15581.

7 H. Feng, B. Wang, N. Wang, J. Qiu, L. Tan and N. Chen, Synthesis and characterization of secondary doped polypyrrole/organic modified attapulgite conductive composite, *J. Appl. Polym. Sci.*, 2015, **132**, 41407–41414.

8 Y. Chen, H. Xu, S. Wang and L. Kang, Removal of Cr(VI) from water using polypyrrole/attapulgite core-shell nanocomposite: equilibrium, thermodynamics and kinetics, *RSC Adv.*, 2014, **4**, 17805–17811.

9 R. Das, S. Giri, A. M. Muliwa and A. Maity, High-performance Hg(II) removal using thiol-functionalized polypyrrole (PPy/MAA) composite and effective catalytic activity of Hg(II)-adsorbed waste material, *ACS Sustainable Chem. Eng.*, 2017, **5**, 7524–7536.

10 X. Du, H. Zhang, X. Hao, G. Guan and A. Abudula, Facile preparation of ion-imprinted composite film for selective electrochemical removal of nickel(II) ions, *ACS Appl. Mater. Interfaces*, 2014, **6**, 9543–9549.

11 R. Seenivasan, W. Chang and S. Gunasekaran, Highly sensitive detection and removal of lead ions in water using cysteine-functionalized graphene oxide/polypyrrole nanocomposite film electrode, *ACS Appl. Mater. Interfaces*, 2015, **7**, 15935–15943.

12 R. Karthik and S. Meenakshi, Chemical modification of chitin with polypyrrole for the uptake of Pb(II) and Cd(II) ions, *Int. J. Biol. Macromol.*, 2015, **78**, 157–164.

13 V. Srivastava, P. Maydannik, Y. C. Sharma and M. Sillanpää, Synthesis and application of polypyrrole coated tenorite nanoparticles (PPy@TN) for the removal of the anionic food dye 'tartrazine' and divalent metallic ions viz. Pb(II), Cd(II), Zn(II), Co(II), Mn(II) from synthetic wastewater, *RSC Adv.*, 2015, **5**, 80829–80843.

14 S. Yang, Z. Li, Y. Wang, X. Fan, Z. Miao, Y. Hu, Z. Li, Y. Sun, F. Besenbacher and M. Yu, Multifunctional Bi@PPy-PEG core-shell nanohybrids for dual-modal imaging and photothermal therapy, *ACS Appl. Mater. Interfaces*, 2018, **10**, 1605–1615.

15 J. Xing, C. Zhu, I. Chowdhury, Y. Tian, D. Du and Y. Lin, Electrically switched ion exchange based on polypyrrole and carbon nanotube nanocomposite for the removal of chromium(VI) from aqueous solution, *Ind. Eng. Chem. Res.*, 2018, **57**, 768–774.

16 W. Fang, X. Jiang, H. Luo and J. Geng, Synthesis of graphene/SiO_2@polypyrrole nanocomposite and their application for Cr(VI) removal in aqueous solution, *Chemosphere*, 2018, **197**, 594–602.

17 Y. Yang, N. Chen, C. Feng, M. Li and Y. Gao, Chromium removal using a magnetic corncob biochar/polypyrrole composite by adsorption combined with reduction: reaction pathway and contribution degree, *Colloids Surf., A*, 2018, **556**, 201–209.

18 J. Chen, X. Hong, Q. Xie, D. Li and Q. Zhang, Sepiolite fiber oriented-polypyrrole nanofibers for efficient chromium(VI) removal from aqueous solution, *J. Chem. Eng. Data*, 2014, **59**, 2275–2282.

19 W. Sun, Y. Zhou, Q. Su, L. Chen, Y. Wang, J. Liu, Y. Sun and H. Ma, Removal of chromium(VI) from aqueous solutions using polypyrrole-based magnetic composites, *Polym. Bull.*, 2017, **74**, 1157–1174.

20 W. Sun, Y. Zhou, J. Liu, Y. Wang, L. Chen and Z. Tian, Polypyrrole/$NiFe_2O_4$ composites with improved hexavalent chromium removal from aqueous solution, *Polym. Compos.*, 2017, **38**, 2779–2787.

21 Z. L. Mo, C. Zhang, R. B. Guo, S. J. Meng and J. X. Zhang, Synthesis of Fe_3O_4 nanoparticles using controlled ammonia vapor diffusion under ultrasonic irradiation, *Ind. Eng. Chem. Res.*, 2011, **50**, 3534–3539.

22 J. Chen, J. Feng and W. Yan, Influence of metal oxides on the adsorption characteristics of PPy/metal oxides for methylene blue, *J. Colloid Interface Sci.*, 2016, **475**, 26–35.

23 X. Wang, T. Wang, D. Liu, J. Guo and P. Liu, Synthesis and electrochemical performance of CeO_2/PPy nanocomposite: interfacial effect, *Ind. Eng. Chem. Res.*, 2016, **55**, 866–874.

24 S. Rascón-Leon, M. M. Castillo-Ortega, I. Santos-Sauceda, G. T. Munive, D. E. Rodriguez-Felix, T. D. Castillo-Castro, J. C. Encinas, J. L. Valenzuela-García, J. M. Quiroz-Castillo, B. García-Gaitan, P. J. Herrera-Franco, J. Alvarez-Sanchez, J. Z. Ramírez and L. S. Quiroz-Castillo, Selective adsorption of gold and silver in bromine solutions by acetate cellulose composite membranes coated with polyaniline or polypyrrole, *Polym. Bull.*, 2017, **75**(7), 3241–3265.

25 J. Feng, N. Sun, D. Wu, H. Yang, H. Xu and W. Yan, Preparation of Fe_3O_4/TiO_2/polypyrrole ternary magnetic composite and using as adsorbent for the removal of acid red G, *J. Polym. Environ.*, 2017, **25**, 781–791.

26 A. Batool, F. Kanwal, M. Imran, T. Jamil and S. A. Siddiqi, Synthesis of polypyrrole/zinc oxide composite and study of their structural, thermal and electrical properties, *Synth. Met.*, 2012, **161**, 2753–2758.

27 B. Mu and A. Wang, One-pot fabrication of multifunctional superparamagnetic attapulgite/Fe_3O_4/polyaniline nanocomposite served as an adsorbent and catalyst support, *J. Mater. Chem. A*, 2015, **3**, 281–289.

28 H. Shen, S. Pan, Y. Zhang, X. Huang and H. Gong, A new insight on the adsorption mechanism of amino-functionalized nano-Fe_3O_4 magnetic polymers in Cu(II), Cr(VI) co-existing water system, *Chem. Eng. J.*, 2012, **183**, 180–191.

29 J. Wang, N. Chen, M. Li and C. Feng, Efficient removal of fluoride using polypyrrole-modifed biochar derived from slow pyrolysis of pomelo peel: sorption capacity and mechanism, *J. Polym. Environ.*, 2018, **26**, 1559–1572.

30 Y. Qi, M. Jiang, Y. Cui, L. Zhao and X. Zhou, Synthesis of quercetin loaded nanoparticles based on alginate for Pb(II) adsorption in aqueous solution, *Nanoscale Res. Lett.*, 2015, **10**, 408–416.

31 M. Maruthapandi, V. B. Kumar, J. H. T. Luong and A. Gedanken, Kinetics, isotherm, and thermodynamic studies of methylene blue adsorption on polyaniline and polypyrrole macro-nanoparticles synthesized by C-dot-initiated polymerization, *ACS Omega*, 2018, **3**, 7196–7203.

32 D. Tang and G. Zhang, Efficient removal of fluoride by hierarchical Ce-Fe bimetal oxides adsorbent: thermodynamics, kinetics and mechanism, *Chem. Eng. J.*, 2015, **283**, 721–729.

33 N. A. S. A. Reyad, Using polypyrrole nanocomposite coated on rice husk ash for the removal of anions, heavy metals, COD from textile wastewater, *HBRC J.*, 2017, **13**, 297–301.

34 Y. Zhan, X. Wan, S. Hea and Y. He, Sulfonated poly(arylene ether nitrile)/polypyrrole core/shell nanofibrous mat: an efficient absorbent for the removal of hexavalent chromium from aqueous solution, *J. Chem. Technol. Biotechnol.*, 2018, **93**, 1432–1442.

35 D. Xu, K. Zhu, X. Zheng and R. Xiao, Poly(ethylene-co-vinyl alcohol) functional nanofiber membranes for the removal of Cr(VI) from water, *Ind. Eng. Chem. Res.*, 2015, **54**, 6836–6844.

36 M. M. Ayad, W. A. Amer, S. Zaghlol, I. M. Minisy, P. Bober and J. Stejskal, Polypyrrole-coated cotton textile as adsorbent of methylene blue dye, *Chemurg. Pap.*, 2018, **72**, 1605–1618.

37 T. S. Anirudhan, P. L. Divya and J. Nima, Utilization of polypyrrole coated iron-doped titania based hydrogel for the removal of tetracycline hydrochloride from aqueous solutions: adsorption and photocatalytic degradation studies, *Environmental Nanotechnology, Monitoring & Management*, 2015, **4**, 106–117.

38 B. Mu, Y. Kang and A. Wang, Preparation of a polyelectrolyte-coated magnetic attapulgite composite for the adsorption of precious metals, *J. Mater. Chem. A*, 2013, **1**, 4804–4811.

39 U. O. Aigbea, R. Dasb, W. H. Hoc, V. Srinivasua and A. Maity, A novel method for removal of Cr(VI) using polypyrrole magnetic nanocomposite in the presence of unsteady magnetic fields, *Sep. Purif. Technol.*, 2018, **194**, 377–387.

40 X. Peng, W. Zhang, L. Gai, H. Jiang, Y. Wang and L. Zhao, Dedoped Fe_3O_4/PPy nanocomposite with high anti-interfering ability for effective separation of Ag(I) from mixed metal-ion solution, *Chem. Eng. J.*, 2015, **280**, 197–205.

41 A. Rengaraj, Y. Haldorai, P. Puthiaraj, S. K. Hwang, T. Ryu, J. Shin, Y.-K. Han, W.-S. Ahn and Y. S. Huh, Covalent triazine polymer-Fe_3O_4 nanocomposite for strontium ion, removal from seawater, *Ind. Eng. Chem. Res.*, 2017, **56**, 4984–4992.